Effects of Mechanical Alignment Errors on Compton Scatter Imaging

Y. F. Du[1], Z. He, G. F. Knoll, D. K. Wehe
Department of Nuclear Engineering and Radiological Science
The University of Michigan, Ann Arbor, MI 48109, USA

Abstract

The development of a prototype Compton scattering camera based on two 1 cm^3 cubic 3-D position sensitive CZT detectors is underway in our laboratory. As a practical problem, the mechanical alignment error may be larger than the 1 mm detector position resolution. This paper investigates the effects of any possible mechanical alignment error on the reconstructed images by Monte Carlo simulations. Our simulation results show that a minor misalignment can cause a significant distortion in the reconstructed image. Any alignment error will lead to a systematic error if the mechanical misalignment is not compensated for. Since the alignment error can cause a distinguishable distortion, system parameters can be adjusted during the image reconstruction procedure until an optimal image is obtained. In this manner, the mechanical alignment error can be automatically determined and compensated for. Our results indicate that any distortion due to alignment error can be eliminated and ensure the angular resolution remains only limited by the two detectors energy and position resolutions.

I. Introduction

Compton cameras have potential applications as radiation imagers in environmental remediation, surveys at nuclear industrial sites, nuclear treaty verification, and medical imaging. These applications are best served by portable devices. However, previous Compton cameras have employed high purity germanium (HPGe), or silicon detectors combined with scintillation detectors. Their portability is limited by the requirement for cryogenic cooling of the semiconductor detectors, and the relatively large volume of the photomultiplier tubes. In contrast, CZT detectors can be operated at room temperature, can achieve high energy and position resolution compared with scintillation detectors, and can be made compact. 3-D position sensitive CZT detectors have been recently demonstrated with a 1.7% FWHM energy resolution at 662 keV and a 1 mm position resolution. They are attractive for portable Compton scattering cameras in the energy region of several hundred keV to a few MeV.

The development of a prototype Compton scattering camera based on two 1 cm^3 cubic 3-D position sensitive CZT detectors is underway in our laboratory. Due to wire bonding requirements between the pixelated detectors and the VA readout chips, the detector is first mounted on a hybrid board, then the whole system is housed in an instrument box. Because of this packaging of the detectors, the alignment error between the two detectors may be larger than the 1 mm detector position resolution. In this paper, effects of any possible mechanical alignment error on the final reconstructed images are investigated by Monte Carlo simulation. An automatic approach to calibrate the alignment error is proposed and tested using Monte Carlo simulated data.

[1]Corresponding author email: yfdu@engin.umich.edu

II. System Overview

As shown in Figure 1, the proposed prototype Compton scattering camera is composed of two 1 cm^3 cubic 3-D position sensitive CZT detectors. There are 11×11 pixels on each anode surface. The signals from the anode pixels are read out by integrated VA chips with independent signal processing channels. For each γ interaction, the energy and lateral (x,y) position information are determined by the anode pixel signal, and the depth (z) information is given by the ratio of the signals from the cathode and the anode pixel. More details about 3-D position sensitive CZT detectors are given in Ref. [1]. Since there is only one second detector for this prototype Compton scattering camera, the whole system or the second detector must rotate around the z axis of the first detector for adequate sampling.

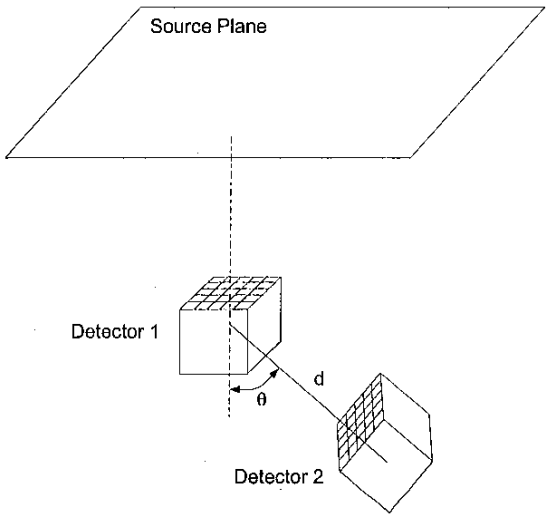

Figure 1: The prototype Compton camera system setup.

In Compton scatter imaging, the incident radiation Compton scatters in the first detector and the scattered photon is detected by the second detector. The source location can be backprojected to lie on the surface of a cone. The cone's axis is defined by the interaction locations in the two detectors, and

the cone angle θ is determined from the Compton equation as:

$$cos(\theta) = 1 - \frac{m_e c^2 E_e}{E_0^2 - E_0 E_e}, \quad (1)$$

where E_0 is the incident energy (assumed known), E_e is the energy deposited in the first detector and m_e is the electron mass. Any energy uncertainty for E_e due to either the first detector energy resolution or the Doppler broadening effect[2, 3, 4], as well as any measurement position uncertainty, will lead to an angular uncertainty of the source location. The overall angular resolution is the quadratic summation of contributions from these three components[5].

Using energy resolutions from currently available detectors, the energy resolution contribution to the angular resolution is larger than 15° for all scattering angles at 114 keV[6]. Thus, the CZT detector is not a good choice for the first detector for low energy Compton scatter imaging. But as shown in Figure 2 for

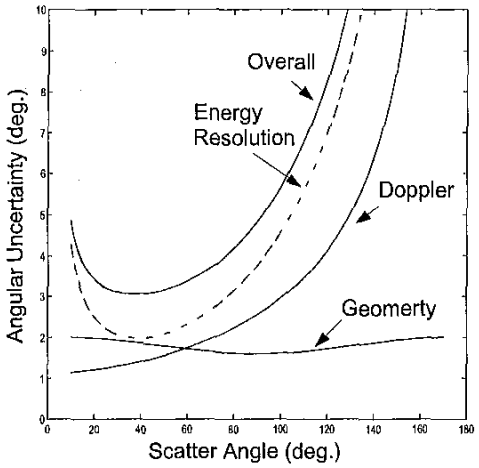

Figure 2: Angular uncertainty estimation at 511 keV.

511 keV gamma rays, the energy resolution contribution to the angular resolution is only $2° - 3°$ for scattering angles between $20° - 80°$, and the Doppler broadening contribution is smaller than 2° for the same scatter angle range. These contributions to angular resolution decrease as the incident energy increases, so currently available CZT detectors can be used in Compton scatter imaging of gamma rays above 500 keV.

The geometric contribution to the angular uncertainty is approximately inversely proportional to the distance between the two detectors. Since Compton camera efficiency is inversely proportional to the square of this distance, there is a tradeoff between the efficiency and the angular resolution. A reasonable choice is to choose the detector separation d such that the geometric contribution is equal to the energy uncertainty contribution. This yields a good efficiency while the overall angular resolution is only $\sqrt{2}$ worse than that determined solely by energy uncertainty. As shown in Figure 2, when the separation distance between two voxels is 4 cm, the geometry contribution is comparable to the detector energy resolution and Doppler broadening contributions. We chose the center-to-center distance between two CZT detectors to be 5 cm so that the distance between the nearest voxels is 4 cm.

As shown in Figure 2, the overall angular resolution is $3° - 4°$ at 511 keV for scattering angles $20° - 80°$. We chose the offset angle θ between the two detectors to be 50°. Corresponding to $20° - 80°$ scattering angles, the field of view (FOV) will be $\pm 30°$ around the axis of the first detector.

Since there are $11 \times 11 \times 20$ voxels in each detector, the memory required to store the coincident spectra and the system response matrix is prohibitively large. As a result, list-mode maximum likelihood[7] is used as the reconstruction algorithm for this prototype Compton scattering camera.

III. Effects of Mechanical Alignment Errors

As shown in Figure 3, the relative position and orientation

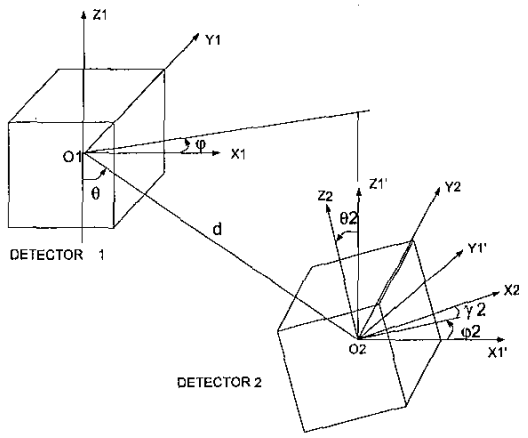

Figure 3: Parameters to describe the relative positions between the two detectors.

of the two detectors can be described by six parameters: the center position of the second detector in the coordinate of the first detector (d, θ, ϕ) and the three Euler angles of the orientation of the second detector $(\theta 2, \phi 2, \gamma 2)$. The mechanical alignment errors between the two detectors can thus be expressed in terms of the difference between the actual and intended values of these six parameters.

As it presented in Section II, the distance d between the two detectors is 5 cm, and the offset scattering angle θ between them is 50°. ϕ can be arbitrarily chosen as 0°. In order to have a more uniform stopping power of the scattered photons in the second detector and to minimize the contribution to the angular resolution of the depth position resolution of the second detector, the top surface of the second detector is angled towards the center of the first detector, i.e., $\theta_2 = 50°, \phi_2 = -90°, \gamma_2 = 90°$.

In order to identify the effects of any possible alignment error of these six parameters, the Monte Carlo program EGS4 is used to generate simulated data. Gaussian noise

with a corresponding FWHM for interaction positions and deposited energy are added to the simulated data to simulate measurement noise. For three 662 keV point sources located at (0,0) cm, (4.0, 0) cm and (0,4.0) cm on a source plane 10 cm from the top of the first detector, the reconstructed images from the Monte Carlo simulated data are shown in Figure 4. During

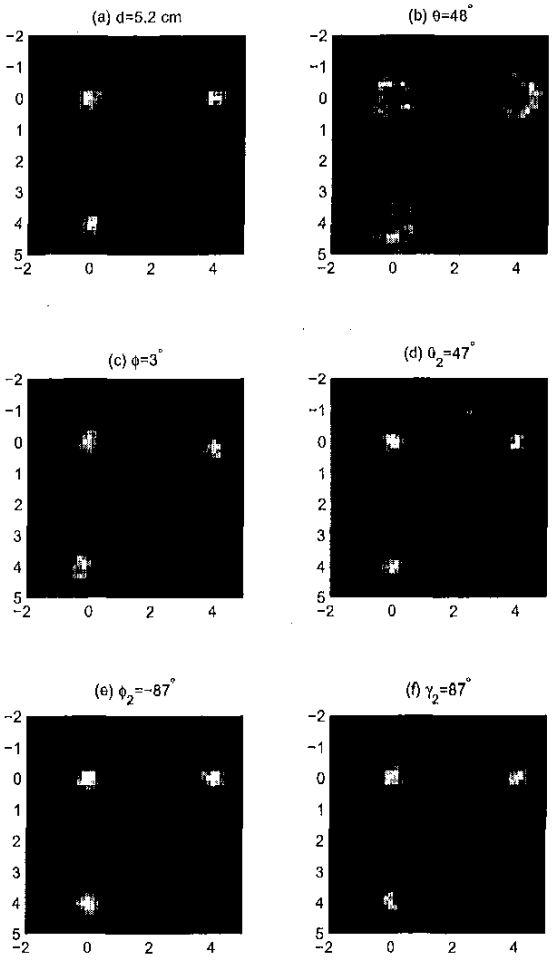

Figure 4: Effects of alignment error of the six parameters which define the relative relationship between two detectors.

the data simulation for each of the six images in Figure 4, a small error was introduced in only one of the six parameters (the perturbed value is shown). While the other five parameters remained exact. In this way, the effect of each parameter can be identified.

From Figure 4, it is clear that the alignment error of the offset angle θ between two detectors causes the largest distortion in the reconstructed image. The reconstructed image spreads out around the true source locations when θ is only 2° less than its design value. When ϕ has a 3° alignment error, each point source has the expected spatial resolution, but the whole reconstructed source plane is rotated by a small angle around the origin. For a small error in the other four parameters, there are no distinguishable distortions in the reconstructed images in Figure 4.

IV. Calibration of Mechanical Alignment Errors

As demonstrated in Figure 4, even a 2° or 3° misalignment in θ or ϕ can cause a distinguishable distortion in the final reconstructed images. In order to ensure the intrinsic spatial resolution determined by the detectors' energy and spatial resolution can be obtained, either these alignment errors must be negligibly small or the alignment error must be known and compensated for during the image reconstruction procedure.

Once the mechanical alignment between the two detectors is fixed, any alignment error will lead to a systematic error in the reconstructed image. This is different from the random noise caused by the measurement energy and position noises. As long as the alignment error causes a distinguishable distortion, system parameters can be adjusted during the image reconstruction procedure until an optimal image is obtained. In this manner, the mechanical alignment error can be automatically determined and compensated for.

In order to test the feasibility of the automatic calibration procedure outlined above, simulation data are generated by EGS4 with following geometry parameters: d=5.2 cm, $\theta = 48°$, $\phi = 3°$, $\theta_2 = 50°$,$\phi_2 = -87°$, $\gamma_2 = 87°$. Note there is a small misalignment in each parameter to simulate a general situation that might occur in practice. The reconstructed image is shown in Figure 5. Although there are misalignments

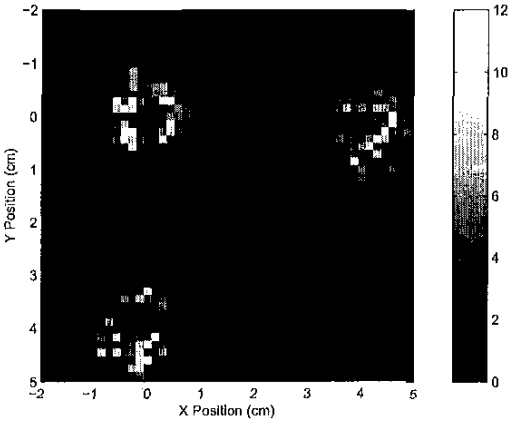

Figure 5: Reconstructed image with a misalignment for each parameter at the same time.

for all six parameters in Figure 5, the image distortion is predominately the combined effect for θ and ϕ illustrated in Figure 4. Thus, the calibration begins with θ, the dominant factor in image distortion. The search range can be set around the design value and ranges to the largest expected alignment error. The reconstructed images with θ from 46° to 51° are shown in Figure 6. The point spread function (PSF)

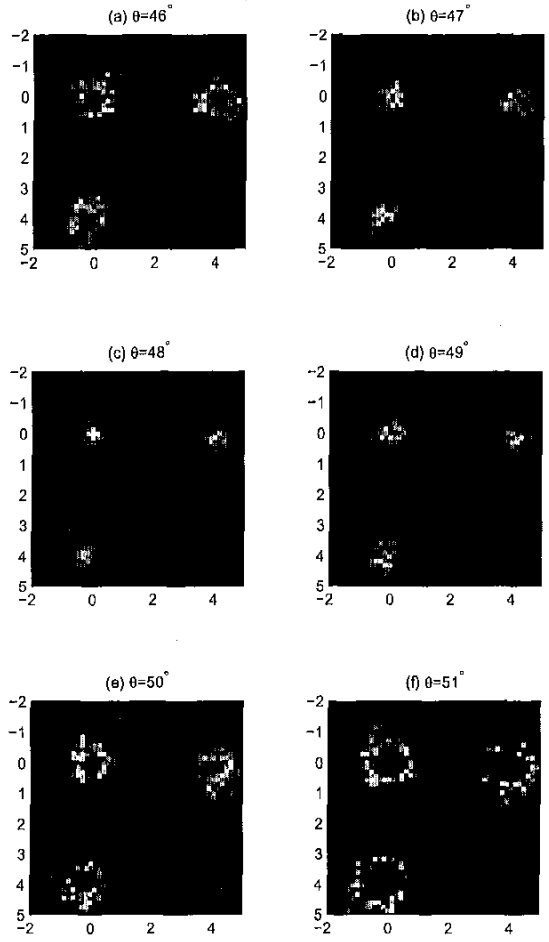

Figure 6: Reconstructed images with θ from 46° to 51°.

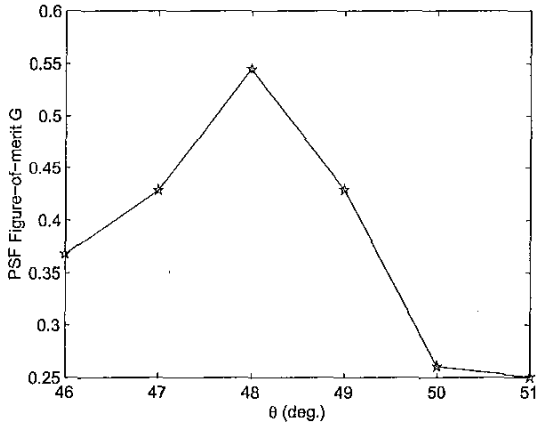

Figure 7: The figure-of-merit G for the point source at the origin in Figure 6.

figure-of-merit[2] G for the point source at the origin can be used to quantitatively measure the reconstructed image. The PSF figure-of-merit G for the source at the origin is shown in Figure 7. From Figures 6 and 7, it is clear that the best image is obtained with $\theta = 48°$, which is the true value of θ in the simulated geometry. Having found θ, a similar search is now conducted for ϕ. The reconstructed images for ϕ from $-1°$ to $4°$ are shown in Figure 8. The centroid y position for a point

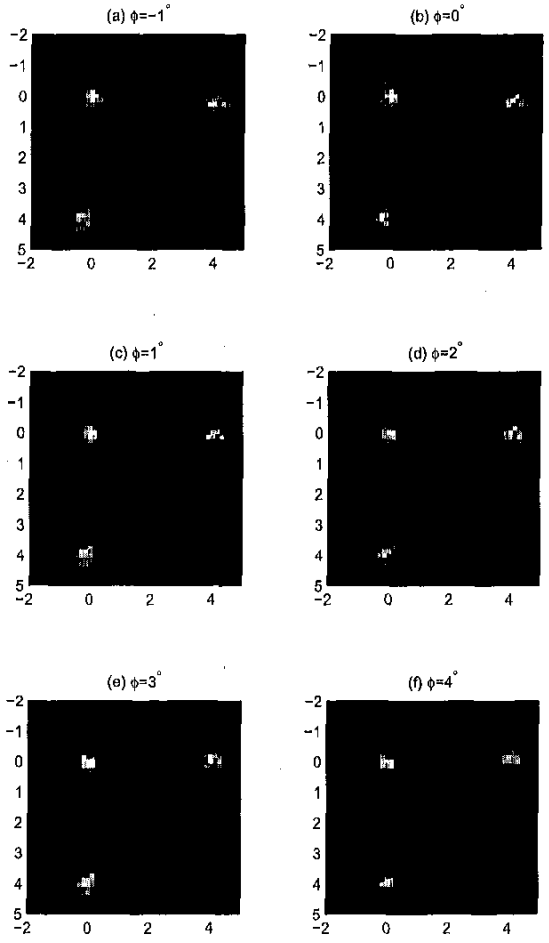

Figure 8: Reconstructed images with ϕ from $-1°$ to $4°$.

source at (4.0,0) and the centroid x position for a point source at (0,4.0) in the reconstructed images are shown in Figure 9. From Figures 8 and 9, it is clear that the image rotation is eliminated when $\phi = 3°$.

Using this two step search procedure over θ and ϕ, their alignment errors can be effectively calibrated even with

[2]PSF figure-of-merit G is defined as [8] $G = \frac{max[f(n_1,n_2)]}{\left[\sum_{n1}\sum_{n2}|f(n_1,n_2)|^2\right]^{(1/2)}}$, where n_1, n_2 are 2-D pixel indexes within the PSF. The G incorporates the entire PSF in the resolution measure, unlike FWHM which only gives the resolution along a line. For an ideal delta function PSF, G=1.

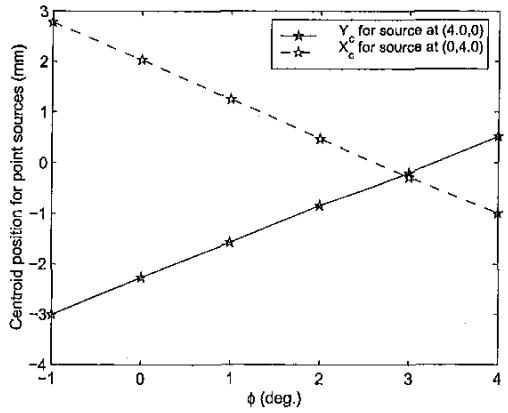

Figure 9: The centroid y position for point source at (4.0,0) and centroid x position for point source at (0,4.0) in Figure 8.

misalignment in the other four parameters. After compensation for the misalignment in θ and ϕ, the final reconstructed image is shown in Figure 8 (e). The source locations have been correctly reconstructed. The FWHM for the on-axis source is 3.2 mm, equivalent to a 1.9° angular resolution. The average FWHM for the two off-axis sources is 4.5 mm, equivalent to 2.6°. Compared with the corresponding predicted angular resolution of 2.7° (at 50° scattering angle) and 3.2° (at 70° scattering angle) for 662 keV gamma rays, the simulation results are slightly better than the predictions. Considering that the simulation does not include the Doppler broadening effects, and using 5 cm separation between the two detectors centers implies the interaction locations for most events will be larger than 4 cm, the simulation and analytical predictions agree well. The key point is that the mechanical misalignment effects are effectively eliminated through this calibration technique.

V. Summary

The effects of mechanical alignment errors of a prototype Compton camera based on two 3-D position sensitive CZT detectors were investigated by Monte Carlo simulations. Our results indicate a minor misalignment can produce a significant distortion in the final reconstructed image. Given the complicated packaging of the detectors, instead of trying to reduce the alignment error between the two detectors with great difficulty, an automatic calibration procedure is proposed. Once the mechanical alignment is fixed, any alignment error causes a systematic error. As long as the alignment errors cause a distinguishable distortion, system parameters can be adjusted during the image reconstruction procedure until an optimal image is obtained. In this manner, the mechanical alignment error can be automatically determined and compensated for. Test results for this prototype Compton camera with Monte Carlo simulated data for a three point source distribution indicates this automatic calibration procedure can effectively determine the alignment errors for major parameters that can cause image distortions. By automatic calibration and compensation, any distortion due to misalignment can be eliminated and ensure the intrinsic angular resolution remains only limited by the two detectors energy and position resolutions.

VI. Acknowledgments

This work is supported under U.S. Department of Energy, Grant No. DE-FG07-98ID13645.

VII. References

[1] Z. He, W. Li, G. F. Knoll, D. K. Wehe, J. Berry, C. M. Stahle, "3-D position sensitive CdZnTe gamma-ray spectrometers", *Nucl. Instr. & Meth.*, A422(1999)173-178.

[2] M. J. Copper, "Compton scattering and electron momentum", *Contemporary Physics*, Vol. 18, No. 5, 1977, pp. 489-517.

[3] R. Cesareo el al., "Interaction of keV photons with matter and new applications", *Physics Reports*, 213, No. 3, 1992, pp. 117-178.

[4] F. Biggs, L. B. Mendelsohn, J. B. Mann, "Hartree-Fock profiles for elements", *Atomic Data and Nuclear Data Tables*, 16, 1975, pp. 201-309.

[5] M. Singh, "An electronically collimated gamma camera for single photon emission computed tomography. Part I: Theoretical consideration and design criteria", *Medical Physics*, Vol. 10, No. 4, 1983 pp. 421-427.

[6] Y. F. Du, Z. He, G. F. Knoll, D. K. Wehe, W. Li, "Evaluation of a Compton Camera using 3-D Position sensitive CdZnTe Detectors", presented at the 44th International Symposium on Optical Science, Engineering and Instrumentation, Denver, Colorado, USA, July 18-23, 1999.

[7] L. Parra, H. H. Barrett, "List-Mode Likelihood: EM algorithm and image quality estimation demonstrated on 2-D PET", *IEEE Transaction on Medical Imaging*, Vol. 17, No. 2, 1998, pp. 228-235.

[8] S. J. Norton and M. Lionzer, "Ultrasonic reflectivity tomography: Reconstruction with circular transducer arrays", *Ultrasonic Imaging*, Vol. 1, 1979, pp. 154-184.